DISCRETE AND CONTINUOUS
DYNAMICAL SYSTEMS
Volume **34**, Number **8**, August **2014**

doi:10.3934/dcds.2014.34.3171

pp. **3171–3182**

PROGRESSIVE WAVES ON A BLUNT INTERFACE

Michael Stiassnie

Faculty of Civil and Environmental Engineering
Technion – Israel Institute of Technology
32000 Haifa, Israel

Raphael Stuhlmeier

Faculty of Mathematics
University of Vienna
Oskar-Morgenstern-Platz 1, 1090 Vienna, Austria

Abstract. We present a new exact solution describing progressive waves on a blunt interface based on Gerstner's trochoidal wave. The second-order irrotational theory is developed for a sharp interface, and subsequently for three fluid layers, the upper and lower of which may approach one another to form the so-called blunt interface. This situation is captured analogously by our exact rotational solution. We establish remarkable agreement between the exact and second-order theories, and present applications to surface water waves.

1. **Introduction.** Mollo-Christensen [12] has shown that Gerstner's [6] exact solution for surface waves can be modified to describe waves on an interface between two fluids; one fluid moving as described by the kinematics of Gerstner waves, and the other fluid in wave-trapped uniform motion moving at the speed of the wave. He also applied this exact finite-amplitude solution to the study of atmospheric billows. Recently Stuhlmeier [13] has applied such a solution to the "dead water" problem.

In the present paper we use a similar approach to obtain an exact solution for a configuration of three layers, where the upper and lower layers move as described by the kinematics of Gerstner waves, and the middle fluid is moving in a wave-trapped uniform motion with the same speed as the waves' celerity. Moreover, we let the middle layer shrink as much as possible, to a configuration which we call a *blunt interface*.

This new exact rotational solution is described in detail in section 4 of the paper. Its irrotational counterpart, accurate to second order in wave steepness, is given in section 3, and is based on the *sharp interface* solution which is outlined in section 2. Comparisons between the rotational and irrotational solutions and some general discussion can be found in section 5.

2. **Internal waves on a sharp interface.** We begin by discussing internal waves on a sharp interface, which we view as perturbations of a *basic flow* of two incompressible inviscid fluids which move in horizontal streams of different velocities and

2010 *Mathematics Subject Classification.* Primary: 76B15; Secondary: 76B55.
Key words and phrases. Internal waves, Gerstner waves, interfacial waves.

densities, one stream above the other. This basic flow is given by velocity, density and pressure:

$$U = \begin{cases} U_u \\ U_l \end{cases} \quad \rho = \begin{cases} \rho_u \\ \rho_l \end{cases} \quad P = \begin{cases} p_0 - g\rho_u y & \text{for } y > 0 \\ p_0 - g\rho_l y & \text{for } y < 0 \end{cases} \tag{2.1}$$

respectively, y is the height, g is the acceleration due to gravity, and p_0 is a constant pressure. We now assume the existence of a wavy motion – a disturbance to the basic flow – given by a velocity potential ϕ on each side of the interface between the two streams:

$$\phi = \begin{cases} U_u x + \phi_u & \text{for } y > \eta, \\ U_l x + \phi_l & \text{for } y < \eta, \end{cases}$$

where the interface itself is given by

$$y = \eta(x, t),$$

x being the horizontal coordinate and t the time.

Both wave potentials have to satisfy the Laplace equation

$$\frac{\partial^2 \phi_u}{\partial x^2} + \frac{\partial^2 \phi_u}{\partial y^2} = 0 \text{ in } y > \eta, \tag{2.2a}$$

$$\frac{\partial^2 \phi_l}{\partial x^2} + \frac{\partial^2 \phi_l}{\partial y^2} = 0 \text{ in } y < \eta. \tag{2.2b}$$

The boundary conditions are as follows:

(a) The wavy motion may be supposed to occur in a finite region so that for all time

$$\nabla \phi \to (U, 0) \text{ as } y \to \pm\infty. \tag{2.3}$$

(b) The kinematic boundary conditions at the interface are

$$\frac{\partial \phi_j}{\partial y} = \frac{\partial \eta}{\partial t} + \left(U_j + \frac{\partial \phi_j}{\partial x} \right) \frac{\partial \eta}{\partial x}, \text{ on } y = \eta, \text{ for } j = u, l;$$

and their Taylor expansions around the basic position $y = 0$ to second order in wave steepness give

$$\frac{\partial \phi_j}{\partial y} - \frac{\partial \eta}{\partial t} - U_j \frac{\partial \eta}{\partial x} = -\frac{\partial^2 \phi_j}{\partial y^2} + \frac{\partial \phi_j}{\partial x} \frac{\partial \eta}{\partial x}, \text{ on } y = 0, \text{ for } j = u, l. \tag{2.4}$$

(c) The dynamic boundary condition of pressure equality, as formulated through Bernoulli's theorem for irrotational flow is

$$\rho_u \left(C_u + \frac{1}{2} U_u^2 + U_u \frac{\partial \phi_u}{\partial x} + \frac{1}{2} \left(\frac{\partial \phi_u}{\partial x} \right)^2 + \frac{1}{2} \left(\frac{\partial \phi_u}{\partial y} \right)^2 + \frac{\partial \phi_u}{\partial t} + gy \right)$$
$$= \rho_l \left(C_l + \frac{1}{2} U_l^2 + U_l \frac{\partial \phi_l}{\partial x} + \frac{1}{2} \left(\frac{\partial \phi_l}{\partial x} \right)^2 + \frac{1}{2} \left(\frac{\partial \phi_l}{\partial y} \right)^2 + \frac{\partial \phi_l}{\partial t} + gy \right), \text{ on } y = \eta,$$

where C_u, C_l are Bernoulli's constants. By virtue of (2.1), these constants must be related by $\rho_u(C_u + U_u^2/2) = \rho_l(C_l + U_l^2/2)$.

The Taylor expansion of the dynamic boundary condition around $y = 0$, to second order in wave steepness, gives

$$\begin{aligned}
&\rho_u\left(U_u\frac{\partial\phi_u}{\partial x}+\frac{\partial\phi_u}{\partial t}+g\eta\right)-\rho_l\left(U_l\frac{\partial\phi_l}{\partial x}+\frac{\partial\phi_l}{\partial t}+g\eta\right)\\
&=-\rho_u\left(U_u\frac{\partial^2\phi_u}{\partial x\partial y}\eta+\frac{1}{2}\left(\frac{\partial\phi_u}{\partial x}\right)^2+\frac{1}{2}\left(\frac{\partial\phi_u}{\partial y}\right)^2+\frac{\partial^2\phi_u}{\partial t\partial y}\eta\right)\\
&+\rho_l\left(U_l\frac{\partial^2\phi_l}{\partial x\partial y}\eta+\frac{1}{2}\left(\frac{\partial\phi_l}{\partial x}\right)^2+\frac{1}{2}\left(\frac{\partial\phi_l}{\partial y}\right)^2+\frac{\partial^2\phi_l}{\partial t\partial y}\eta\right),\ \text{on } y=0. \qquad (2.5)
\end{aligned}$$

For waves of small steepness ε we assume a solution of the form

$$\phi_u=\varepsilon A_{u1}\exp[i(kx-\omega t)-ky]+\varepsilon^2A_{u2}\exp[2i(kx-\omega t)-2ky]+\text{c.c.} \qquad (2.6a)$$

$$\phi_l=\varepsilon A_{l1}\exp[i(kx-\omega t)+ky]+\varepsilon^2A_{l2}\exp[2i(kx-\omega t)+2ky]+\text{c.c.} \qquad (2.6b)$$

$$\eta=\varepsilon B_1\exp[i(kx-\omega t)]+\varepsilon^2B_2\exp[2i(kx-\omega t)]+\text{c.c.} \qquad (2.6c)$$

where ω is the wave frequency, k is the wave-number, and c.c. stands for the complex-conjugate. Note that (2.6a) and (2.6b) satisfy (2.2a) and (2.2b) respectively, as well as (2.3).

Substituting (2.6) into (2.4) and (2.5) and separating linear terms in ε from quadratic terms, leads to the following two systems, each consisting of three linear algebraic equations:

$$i(\omega-kU_u)B_1-kA_{u1}=0, \qquad (2.7a)$$

$$i(\omega-kU_l)B_1+kA_{l1}=0, \qquad (2.7b)$$

$$g(\rho_u-\rho_l)B_1-i\rho_u(\omega-kU_u)A_{u1}+i\rho_l(\omega-kU_l)A_{l1}=0, \qquad (2.7c)$$

and

$$i(\omega-kU_u)B_2-kA_{u2}=-ik(\omega-kU_u)B_1^2, \qquad (2.8a)$$

$$i(\omega-kU_l)B_2+kA_{l2}=ik(\omega-kU_l)B_1^2, \qquad (2.8b)$$

$$\begin{aligned}
&g(\rho_u-\rho_l)B_2-2i\rho_u(\omega-kU_u)A_{u2}+2i\rho_l(\omega-kU_l)A_{l2}\\
&=-i\rho_uk(\omega-kU_u)B_1A_{u1}-i\rho_lk(\omega-kU_l)B_1A_{l1}. \qquad (2.8c)
\end{aligned}$$

Note that (2.7) is homogeneous, whereas the right-hand side of (2.8) is given in terms of the solution of (2.7).

Solving (2.7) first gives A_{u1} and A_{l1} in terms of a freely chosen B_1, as well as the dispersion relation

$$A_{u1}=i(\omega-kU_u)B_1/k, \qquad (2.9a)$$

$$A_{l1}=-i(\omega-kU_l)B_1/k, \qquad (2.9b)$$

$$\rho_u(\omega-kU_u)^2+\rho_l(\omega-kU_l)^2+gk(\rho_u-\rho_l)=0. \qquad (2.9c)$$

Note that the above solution is in full agreement with equations (3.19) and (3.20) of Drazin [5]. Substituting (2.9) into (2.8) and solving yields:

$$A_{u2} = i(\omega - kU_u)\left(\frac{B_2}{k} + B_1^2\right) \tag{2.10a}$$

$$A_{l2} = i(\omega - kU_l)\left(\frac{-B_2}{k} + B_1^2\right) \tag{2.10b}$$

$$B_2 = \frac{\left(\rho_l(\omega - kU_l)^2 - \rho_u(\omega - kU_u)^2\right) B_1^2}{\rho_u\left(2(\omega - kU_u)^2/k + g\right) - \rho_l\left(-2(\omega - kU_l)^2/k + g\right)} \tag{2.10c}$$

This completes the solution for the problem of internal waves on a sharp interface to second order. In the following section we shall use two special cases of the above problem to define a particular three-layer problem, and to provide a new solution for irrotational progressive waves on a blunt interface.

3. **Irrotational progressive waves on a blunt interface.** We approach the problem of waves on a blunt interface by first assuming a basic flow of three horizontal fluid layers, replacing (2.1) by

$$U = \begin{cases} 0 \\ U_m = \omega/k \\ 0 \end{cases} \quad \rho = \begin{cases} \rho_u \\ \rho_m \\ \rho_l \end{cases} \quad P = \begin{cases} p_0 - g\rho_m\delta - g\rho_u(y - \delta) & \text{for } y > \delta \\ p_0 - g\rho_m y & \text{for } -\delta < y < \delta \\ p_0 + g\rho_m\delta - g\rho_l(y + \delta) & \text{for } y < -\delta \end{cases} \tag{3.1}$$

where now the disturbances of the basic flow are given on

$$y = \delta + \eta_u(kx - \omega t) \text{ and } y = -\delta + \eta_l(kx - \omega t), \tag{3.2}$$

the loci of the upper and lower interfaces, respectively, both having the same frequencies and wave-numbers. At each of these we now have a configuration akin to that discussed in section 2. Note that (2.9a, 2.9b) and (2.10a, 2.10b) then guarantee that in the middle layer $\phi = U_m x$ solely.

Applying the dispersion relation (2.9c) to the upper and lower interfaces gives

$$k = g(\rho_m - \rho_u)/\rho_u U_m^2 = g(\rho_l - \rho_m)\rho_l U_m^2 \tag{3.3}$$

which leads to the conclusion that the density of the middle layer must be

$$\rho_m = \frac{2\rho_l\rho_u}{\rho_l + \rho_u}. \tag{3.4}$$

Adding the requirement that B_1 is the same for both interfaces, and using (2.10c) gives for the upper and lower interfaces

$$B_{2u} = -\frac{\rho_u\omega^2 B_1^2}{g(\rho_m - \rho_u)} < 0, \tag{3.5a}$$

$$B_{2l} = \frac{\rho_l\omega^2 B_1^2}{g(\rho_l - \rho_m)} > 0. \tag{3.5b}$$

From (3.5a, 3.5b) and (3.3) one can see that

$$B_{2u} = -B_{2l}.$$

The equations for the upper and lower interface are

$$y = \delta + 2\varepsilon B_1\cos(kx - \omega t) - 2\varepsilon^2 B_{2l}\cos(2(kx - \omega t)),$$

$$y = -\delta + 2\varepsilon B_1\cos(kx - \omega t) + 2\varepsilon^2 B_{2l}\cos(2(kx - \omega t)).$$

Using (3.5b) and (3.4) we obtain

$$B_{2l} = \frac{(\rho_l + \rho_u)\omega^2 B_1^2}{g(\rho_l - \rho_u)},$$

and (3.3) with (3.4) gives

$$\omega^2(\rho_u + \rho_l) = gk(\rho_l - \rho_u). \tag{3.7}$$

Note that the dispersion relation (3.7) is identical to that obtained for a sharp interface when U_u and U_l are set to zero in (2.9c).

In order to obtain an internal wave with a blunt interface we let $\delta \to 2\varepsilon^2 B_{2l}$, and the "interface" becomes the region

$$|y - 2\varepsilon B_1 \cos(kx - \omega t)| \le 2\varepsilon^2 B_{2l}(1 - \cos(2(kx - \omega t)).$$

If one sets $2\varepsilon B_1 = \tilde{a}$ and $kx - \omega t = \theta$, the above may be written in the form

$$\tilde{a}\cos\theta - \frac{k\tilde{a}^2}{2}(1 - cos2\theta) \le y \le \tilde{a}\cos\theta + \frac{k\tilde{a}^2}{2}(1 - cos2\theta) \tag{3.8}$$

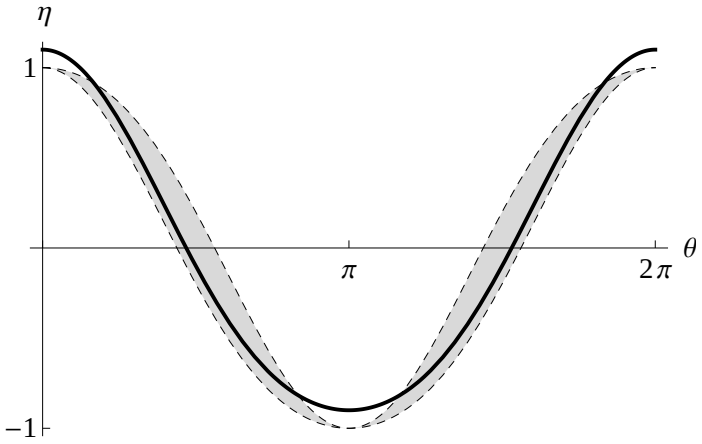

FIGURE 1. The blunt "interface" represented by the shaded area (for $\tilde{a} = 1$, $\tilde{a}k = 0.2$), and a sharp water/air interface (solid curve, $\rho_u = 0.001\rho_l$).

Figure 1 shows this blunt "interface" as the region bounded by the dashed curves for $\tilde{a} = 1$ and $\tilde{a}k = 0.2$. For comparison, the sharp interface, given by

$$y = \tilde{a}\cos\theta + \frac{k\tilde{a}^2}{2}\frac{\rho_l - \rho_u}{\rho_l + \rho_u}\cos 2\theta,$$

is plotted for a representative value of $\frac{\rho_l - \rho_u}{\rho_l + \rho_u} = 0.998$, representing internal waves at a water/air interface.

4. **Rotational progressive waves on a blunt interface.** We now describe explicitly rotational progressive waves on a blunt interface, based on Gerstner's trochoidal solution.

4.1. **Lagrangian governing equations.** As this solution is explicitly derivable only in Lagrangian variables, we introduce to this end the particle markers a and b in a label space $\{(a,b) \in \mathbb{R} \times \mathbb{R}\}$, and describe the paths of the particles via the particle trajectory map

$$(a,b) \mapsto (x(t,a,b), y(t,a,b)).$$

The particle velocities are then given by

$$\dot{x}(t,a,b) = u(x,y,t), \quad \dot{y}(t,a,b) = v(x,y,t).$$

In formulating the governing equations, we relate the derivatives in the Eulerian and Lagrangian frames via

$$\begin{pmatrix} \frac{\partial}{\partial a} \\ \frac{\partial}{\partial b} \end{pmatrix} = \begin{pmatrix} \frac{\partial x}{\partial a} & \frac{\partial y}{\partial a} \\ \frac{\partial x}{\partial b} & \frac{\partial y}{\partial b} \end{pmatrix} \begin{pmatrix} \frac{\partial}{\partial x} \\ \frac{\partial}{\partial y} \end{pmatrix}$$

and

$$\begin{pmatrix} \frac{\partial}{\partial x} \\ \frac{\partial}{\partial y} \end{pmatrix} = \frac{1}{J} \begin{pmatrix} \frac{\partial y}{\partial b} & -\frac{\partial y}{\partial a} \\ -\frac{\partial x}{\partial b} & \frac{\partial x}{\partial a} \end{pmatrix} \begin{pmatrix} \frac{\partial}{\partial a} \\ \frac{\partial}{\partial b} \end{pmatrix}$$

whence it is easy to see that the equation of mass conservation, in Eulerian coordinates (i.e. the condition that the fluid velocity field is divergence free) takes the form

$$\frac{1}{J}\frac{\partial J}{\partial t} = 0$$

where

$$J = \left(\frac{\partial x}{\partial a}\frac{\partial y}{\partial b} - \frac{\partial x}{\partial b}\frac{\partial y}{\partial a} \right)^{-1}.$$

Thus mass conservation is equivalent to the Jacobian of the coordinate transform being independent of time.

Making use of the above relations, we find that the Euler equations take the form

$$\frac{1}{\rho}\frac{\partial p}{\partial a} = -\frac{\partial x}{\partial a}\ddot{x} - \frac{\partial y}{\partial a}(\ddot{y} + g), \tag{4.1}$$

$$\frac{1}{\rho}\frac{\partial p}{\partial b} = -\frac{\partial x}{\partial b}\ddot{x} - \frac{\partial y}{\partial b}(\ddot{y} + g), \tag{4.2}$$

where p is the pressure. The interfacial kinematic boundary condition amounts to specifying that the interface corresponds to a fixed value of the label b, say $b = b_0$, while the dynamic boundary condition means that the pressure must be continuous across any such interface.

Within this Lagrangian framework a number of explicit solutions to the incompressible Euler equations have been found; a discussion of classical solutions, as well as some newly discovered ones, may be found in Aleman and Constantin [1].

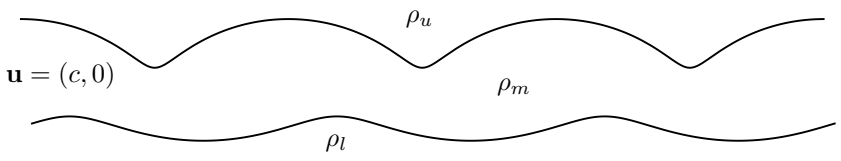

FIGURE 2. The three-layer fluid domain.

4.2. **Form and properties of the three-layer solution.** Figure 2 depicts the configuration of our three-fluid domain, and in what follows, we shall use suffixes u, m and l to denote variables of the *upper, middle* and *lower* flows, respectively, when needed for clarity. The wave motion in the lower layer is given by

$$\begin{cases} x = a + \frac{e^{kb}}{k} \sin k(a - ct) \\ y = -\Delta + b - \frac{e^{kb}}{k} \cos k(a - ct) \end{cases} \qquad a \in \mathbb{R},\ b \leq b_l \leq 0, \tag{4.3}$$

that of the upper layer is

$$\begin{cases} x = a + \frac{e^{-kb}}{k} \sin k(a - ct + \alpha) \\ y = \Delta + b + \frac{e^{-kb}}{k} \cos k(a - ct + \alpha) \end{cases} \qquad a \in \mathbb{R},\ b \geq b_u \geq 0, \tag{4.4}$$

while the intermediate layer – which may be interpreted as our blunt interface for suitable choice of Δ, as we shall see below – is the region

$$-\Delta + b_l - \frac{e^{kb_l}}{k} \cos k(a - ct) \leq y \leq \Delta + b_u + \frac{e^{-kb_u}}{k} \cos k(a - ct + \alpha) \tag{4.5}$$

moves with a uniform velocity $(u, v) = (c, 0)$ (cf. (3.2)). Here $c = \omega/k$ is the celerity of the waves, α is an as yet arbitrary phase shift, and Δ is a vertical translation.

We can clearly see by (4.3) that a particle labelled by (a, b) moves clockwise along a circular path around $(a, b - \Delta)$ with radius e^{kb}/k, while a particle in the upper domain (4.4) moves counter-clockwise about $(a, b + \Delta)$. The upper and lower domains exhibit a non-vanishing vorticity Ω_u, Ω_l which decays exponentially with distance from the interface,

$$\Omega_l = \frac{2cke^{2kb}}{1 - e^{2kb}} > 0,$$
$$\Omega_u = \frac{-2cke^{-2kb}}{1 - e^{-2kb}} < 0,$$

and which may be seen to become infinite for the cusped wave with $b_i = 0$, $i \in \{u, l\}$.

In order to elucidate the structure of the interface, we shall switch to a frame of reference moving with the wave celerity: $-c$, so that the motion becomes steady and the profiles fixed, and denote by $k(a - ct) = \vartheta$. Then the lower motion (4.3) is

$$\begin{cases} x = \frac{\vartheta}{k} + \frac{e^{kb}}{k} \sin \vartheta \\ y = -\Delta + b - \frac{e^{kb}}{k} \cos \vartheta \end{cases}$$

which upon fixing b is seen to be the curve of a trochoid; that is, the curve $b_l (\leq 0)$ is traced by a point situated a distance e^{kb_l}/k from the center of a circle of radius $1/k$ as that circle rolls below the line $y = b_l - \Delta + \frac{1}{k}$.

Analogously, the upper wave motion (4.4) is reduced via the same "artifice of steady motion" [9] to

$$\begin{cases} x = \frac{\vartheta}{k} + \frac{e^{-kb}}{k} \sin(\vartheta + k\alpha) \\ y = \Delta + b + \frac{e^{-kb}}{k} \cos(\vartheta + k\alpha) \end{cases}$$

whereupon the the curve described by fixing $b = b_u \geq 0$ may be seen to be the trochoid traced by a point a distance e^{-kb_u}/k from the center of a circle of radius $1/k$ as that circle rolls on top of the line $y = b_u + \Delta - 1/k$.

In both cases, the assumption $b_l \leq 0$ respectively $b_u \geq 0$ is necessary to prevent self intersection of these curves, and the limiting cases $b_i = 0$, $i \in \{l, u\}$, correspond to the cusped trochoid, also known as a cycloid. For arbitrary α we may assume

$\Delta > 1/2((b_l + e^{kb_l}/k) - (b_u - e^{-kb_u}/k))$ to ensure that the intermediate region remains simply connected.

4.3. **Verification of the governing equations.** It is straightforward to verify the condition of mass conservation for the flows described by (4.3) and (4.4). The Jacobian determinant of the lower layer flow (4.3) is seen to be $J = 1 - e^{2kb}$, while that of the upper flow (4.4) is $J = 1 - e^{-2kb}$, both of which are time-independent.

We have seen that the two interfaces bounding the middle layer (4.5) from above and below are given by specifying a value of b. As these interfaces describe traveling waves, we may write them in an Eulerian framework as $\eta_i(x - ct)$, $i \in \{l, u\}$, whereupon the kinematic boundary condition can be satisfied only when the middle layer moves in wave-trapped uniform motion, i.e. its Eulerian velocity field is $(u, v) = (c, 0)$, mirroring (3.1).

We see that the right hand sides of the Euler equations (4.1) and (4.2) may be computed explicitly. For the lower wave domain, this yields a pressure

$$p_l = -\rho_l \left((c^2 k - g) \frac{e^{kb}}{k} \cos k(a - ct) - \frac{c^2}{2} e^{2kb} + gb \right) + C_l. \tag{4.7}$$

The Euler equations are satisfied for the upper wave domain with a pressure given by

$$p_u = -\rho_u \left(gb - \frac{c^2}{2} e^{-2kb} + (c^2 k + g) \frac{e^{-kb}}{k} \cos k(a - ct + \alpha) \right) + C_u. \tag{4.8}$$

It remains to resolve the issue of continuity of the pressure, and we shall see that this will be a central one in determining characteristics of our problem. We see that (4.7) must match the pressure of the middle layer at $y = -\Delta + b_l - \frac{e^{kb_l}}{k} \cos k(a - ct)$, while (4.8) must match this pressure at $y = \Delta + b_u + \frac{e^{-kb_u}}{k} \cos k(a - ct + \alpha)$. Since the intermediate layer is in uniform motion, the pressure therein may be given by $p_m = -g\rho_m y + p_0$ for some constant p_0. For the lower Gerstner flow (4.3), the condition that the pressure be continuous at all times implies the dispersion relation

$$c^2 k = g \frac{\rho_l - \rho_m}{\rho_l},$$

while for the upper Gerstner flow (4.4) one obtains the dispersion relation

$$c^2 k = g \frac{\rho_m - \rho_u}{\rho_m},$$

where the right hand side may in both cases be interpreted as a *reduced gravity*. Remarkably, these dispersion relations coincide exactly with those found from the irrotational theory (3.3). As in the irrotational problem presented in section 3, we assume the upper and lower waves in our exact, rotational problem have the same frequency and wave-number, which fixes the density of the middle layer as in (3.4). The dispersion relation for our waves can then be expressed as

$$c^2 k = g \left(\frac{\rho_l - \rho_u}{\rho_l + \rho_u} \right). \tag{4.10}$$

The matching of pressures at the lower interface furthermore requires

$$g\rho_l \left(\frac{\rho_l - \rho_u}{\rho_l + \rho_u} \right) \left(\frac{1}{2k} e^{2kb_l} - b_l \right) = p_0 - C_l + g\Delta \frac{2\rho_u \rho_l}{\rho_l + \rho_u},$$

and at the upper interface, analogously,

$$g\rho_u\left(\frac{\rho_l-\rho_u}{\rho_l+\rho_u}\right)\left(\frac{1}{2k}e^{-2kb_u}+b_u\right)=p_0-C_u-g\Delta\frac{2\rho_u\rho_l}{\rho_l+\rho_u},$$

which fixes the constants C_l, C_u. This completes our verification that the new solution satisfies all governing equations exactly.

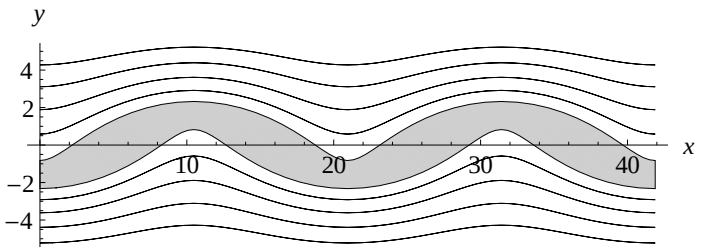

FIGURE 3. Plot of the full explicit internal-wave solution ($k\alpha=\pi$, $b_l=-b_u=-3.5$, $k=0.3$, $\Delta=1.75$). The co-moving intermediate layer is depicted as the shaded region.

4.4. **Rotational waves on a blunt interface.** The upper and lower Gerstner waves can be readily seen to be in phase for $k\alpha=2\pi\kappa$, $\kappa\in\mathbb{Z}$ and out of phase for $k\alpha=(2\kappa+1)\pi$, $\kappa\in\mathbb{Z}$. It is this latter case that interests us for the study of the exact blunt-interface problem. The upper and lower interfaces can then be shifted towards each other and made to meet at each crest and trough by setting $b_u=-b_l$ and letting $\Delta\to b_l$, which is a non-positive quantity. Figure 3 depicts the exact solution to the three-layer problem – the decay of wave amplitude with distance from the middle layer shown by lines of constant b – the upper and lower waves out of phase and of equal amplitude and steepness.

5. **Discussion.** The similarities between the exact rotational solution and the second-order irrotational solution are striking. It is well known that the limit of the classical Gerstner wave for $b_l\to-\infty$ is the first-order deep-water wave. Indeed the particle trajectories of these two waves are both circular [8]. It is worth noting that circular particle trajectories are a feature of the first order theory, and dissappear at second order (see [3]). Nonclosed trajectories are typical of irrotational, periodic waves when no approximations based on small amplitude are made, whether over a flat bed or in deep water, cf. Constantin [2], Constantin & Strauss [4], and Henry [7].

In our study of internal waves on a blunt interface, we have established noteworthy similarities and in some cases perfect agreement between the exact and the second-order theory in (i) shape, (ii) dispersion relation, (iii) density of the middle layer, and (iv) average thickness of the interface.

Figure 4 shows different forms of the blunt interface, for the exact rotational theory as well as the second-order irrotational theory. Panels 4a–4d show waves with a steepness similar to that of typical ocean surface waves. Panels 4e and 4f depict a steepness of 0.3, approximately the the steepness for which classical Gerstner waves become unstable [10]. Finally, panels 4g and 4h are approximately the steepness of the maximal Stokes wave [11, p. 768]. For waves of small steepness, the agreement between the two theories is notable.

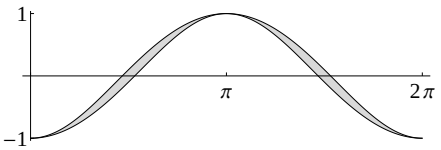

(A) Gerstner internal wave with $k\tilde{a} = 0.1$.

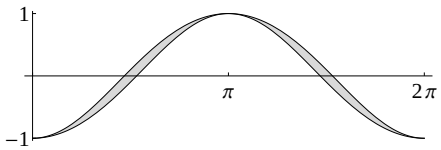

(B) Nonlinear internal wave with $k\tilde{a} = 0.1$.

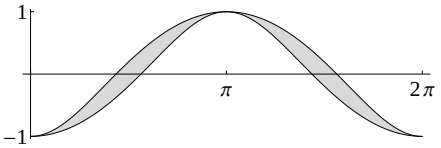

(C) Gerstner internal wave with $k\tilde{a} = 0.2$.

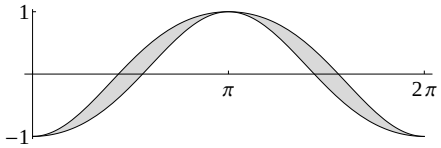

(D) Nonlinear internal wave with $k\tilde{a} = 0.2$.

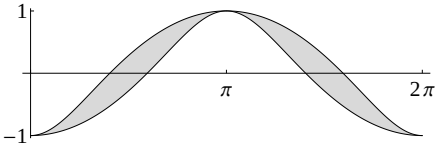

(E) Gerstner internal wave with $k\tilde{a} = 0.3$.

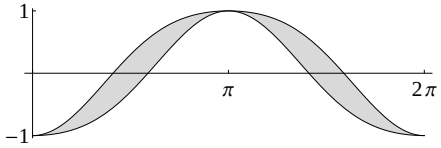

(F) Nonlinear internal wave with $k\tilde{a} = 0.3$.

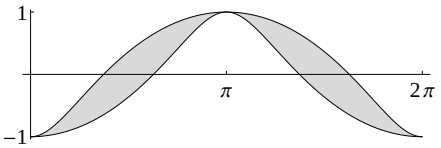

(G) Gerstner internal wave with $k\tilde{a} = 0.4$.

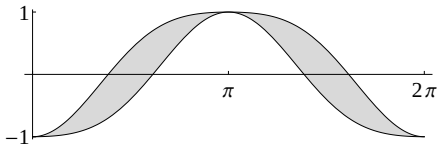

(H) Nonlinear internal wave with $k\tilde{a} = 0.4$.

FIGURE 4. A comparison of the blunt interfaces (see (3.8), (4.5)) given as the shaded areas, illustrated as a function of θ. Presented are the exact rotational theory (left) and the second-order irrotational theory (right) for amplitude $\tilde{a} = 1$ and wavenumbers $k = 0.1, 0.2, 0.3,$ and 0.4.

Indeed, the area of the blunt interface from trough to crest for the exact solution is given by

$$A = \frac{\pi e^{2kb_l}}{k^2} = \pi\tilde{a}^2,\ b_l \leq 0,$$

where $\tilde{a}$ is the amplitude of the Gerstner wave, and decays exponentially to zero with decreasing steepness. The average thickness of the interface is then given by

$$T_{avg} = \frac{e^{2kb_l}}{k} = \frac{2\pi\tilde{a}^2}{\lambda},$$

which is identical with the average thickness of the second-order blunt interface (3.8), and can be seen to tend to zero with decreasing steepness. This latter property is visible in figure 4.

We have also established agreement between the dispersion relations for the exact (4.10) and second-order solutions (3.7). In addition, the density of the middle layer (3.4) in both approaches also coincides.

In the exact theory, the wave motion decays exponentially away from the blunt interface, so that at a distance of one wavelength, the wave amplitudes are reduced to less than 0.2% of their value at the interface.

In contrast to the classical Gerstner wave, which is formulated for a single fluid, and disregards variations in pressure above the trochoidal interface, the exact rotational internal waves presented above no longer exhibit constant pressure along lines of constant b. This feature may be exploited in the classical case to describe Gerstner waves with stratified density, where mass conservation takes the form $\rho_t + u\rho_x + v\rho_y = 0$, and the Gerstner flow implies $\rho_a = 0$, and is thus barotropic. The classical Gerstner wave, a modern discussion of which may be found in Constantin [3], is recovered from our interfacial wave by setting $\rho_u = \rho_m = 0$.

We present some details on interfacial waves between water and air, adapting the blunt-interface solution thereto. In this context, the blunt interface represents the lowermost part of the marine–atmospheric boundary layer with a constant density given by (3.4). In principle, our explicit solution could be extended to arbitrarily many layers, separated by co-moving blunt interfaces (or regions) with a specified celerity and density.

Values of density typical for water and air are

$$\rho_l = 10^3 \text{ kg/m}^3,\ \rho_u = 1.2 \text{ kg/m}^3,$$

while for a prototypical ocean wave we take a wavelength and amplitude of

$$\lambda = 100 \text{ m},\ \tilde{a} = 1 \text{ m}.$$

Our theory yields a blunt interface with an average thickness of just 6 cm, and with a density $\rho_m \approx 2.4$ kg/m^3, twice the density ρ_u of the upper layer of air – which we may attribute to the concentration of droplets of spray a small distance away from the sea-surface. The dispersion relation is modified slightly from that for linear deep water waves when the upper layer is neglected; indeed, we find that our waves propagate at a celerity

$$c = 0.9988 \cdot \sqrt{g/k},$$

which in this case is approximately $c = 12.5$ m/s. Our theoretical considerations are equally applicable to a water/water as well as an air/air interface, provided the boundary condition (2.3) can be suitably justified.

Acknowledgments. The authors are grateful to the anonymous referees for their helpful suggestions. Both authors acknowledge support by ERC Grant NWFV – Nonlinear studies of water flows with vorticity.

REFERENCES

[1] A. Aleman and A. Constantin, Harmonic maps and ideal fluid flows, *Arch. Rat. Mech. Anal.*, **204** (2012), 479–513.

[2] A. Constantin, The trajectories of particles in Stokes waves, *Invent. Math.*, **166** (2006), 523–535.

[3] A. Constantin, *Nonlinear Water Waves with Applications to Wave-Current Interactions and Tsunamis*, SIAM, 2012.

[4] A. Constantin and W. Strauss, Pressure beneath a Stokes wave, *Commun. Pure Appl. Math.*, **63** (2010), 533–557.
[5] P. G. Drazin, *Introduction to Hydrodynamic Stability*, Cambridge University Press, 2002.
[6] F. Gerstner, *Theorie der Wellen Samt Einer Daraus Abgeleiteten Theorie der Deichprofile*, Abhandlungen der kön. böhmischen Gesellschaft der Wissenschaften, 1804.
[7] D. Henry. On the deep-water stokes wave flow. *Int. Math. Res. Not.*, **2008** (2008), 7 pp.
[8] B. Kinsman, *Wind Waves*, Dover, New York, 1984.
[9] H. Lamb, *Hydrodynamics*, Cambridge University Press, Cambridge, 1895.
[10] S. Leblanc, Local stability of Gerstner's waves, *J. Fluid Mech.*, **506** (2004), 245–254.
[11] C. C. Mei, M. Stiassnie and D. K.-P. Yue, *Theory and Applications of Ocean Surface Waves*, World Scientific Publishing Co., 2005.
[12] E. Mollo-Christensen, Gravitational and geostrophic billows: Some exact solutions, *J. Atmos. Sci.*, **35** (1978), 1395–1398.
[13] R. Stuhlmeier, Internal Gerstner waves: Applications to dead water, *Appl. Anal.*, to appear.

Received August 2013; revised September 2013.

E-mail address: miky@technion.ac.il
E-mail address: raphael.stuhlmeier@univie.ac.at